Article:
Tu, Yao Jen, Premachandra, Gnanasiri S., Boyd, Stephen A. et al. (2021) Synthesis and evaluation of Fe3O4-impregnated activated carbon for dioxin removal. CHEMOSPHERE. 128263. ISSN: 0045-6535

https://doi.org/10.1016/j.chemosphere.2020.128263

Graphical Abstract

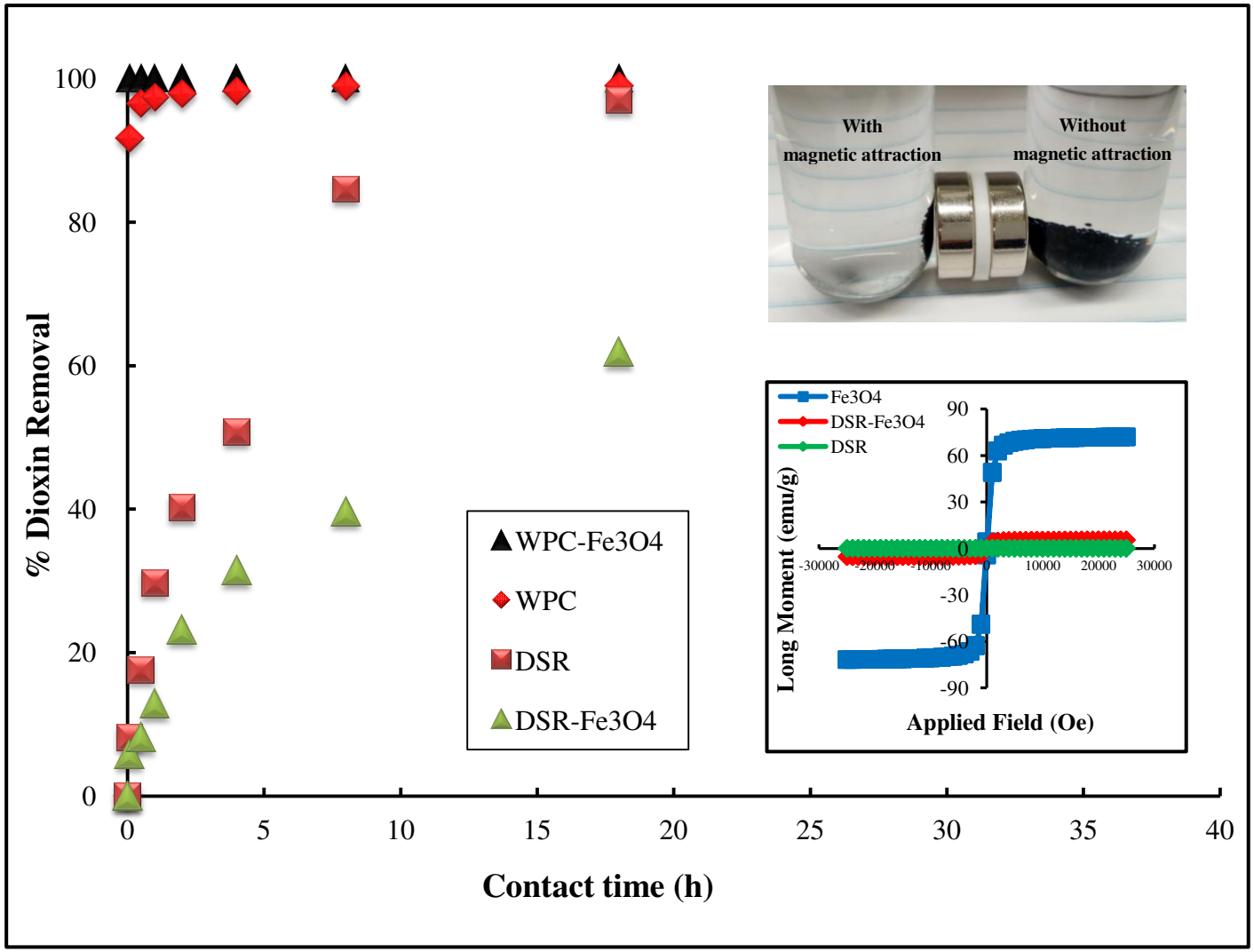

*Title Page

Synthesis and evaluation of Fe_3O_4-impregnated activated carbon for dioxin removal

Yao-Jen Tu[a], Gnanasiri S. Premachandra[b], Stephen A. Boyd[c], J. Brett Sallach[d], Hui Li[c], Brian J. Teppen[c], Cliff T. Johnston[b,e*]

[a] School of Environmental and Geographical Sciences, Shanghai Normal University, 100 Guilin Rd. Shanghai, 200234, China

[b] Department of Agronomy, Purdue University, 915 W. State Street, West Lafayette, Indiana 47907, USA

[c] Department of Plant, Soil, and Microbial Sciences, Michigan State University, East Lansing, Michigan, 48824, USA

[d] Department of Environment and Geography, University of York, Heslington, York, YO10 5NG, UK

[e] Department of Earth, Atmospheric and Planetary Sciences, 550 Stadium Mall, Purdue University, West Lafayette, IN 47907, USA

Corresponding author: Cliff T. Johnston

Fax: +1-7654961716

E-mail: cliffjohnston@purdue.edu

Synthesis and evaluation of Fe_3O_4-impregnated activated carbon for dioxin removal

Yao-Jen Tu[a], Gnanasiri S. Premachandra[b], Stephen A. Boyd[c], J. Brett Sallach[d], Hui Li[c], Brian J. Teppen[c], Cliff T. Johnston[b,e*]

[a] School of Environmental and Geographical Sciences, Shanghai Normal University, 100 Guilin Rd. Shanghai, 200234, China

[b] Department of Agronomy, Purdue University, 915 W. State Street, West Lafayette, Indiana 47907, USA

[c] Department of Plant, Soil, and Microbial Sciences, Michigan State University, East Lansing, Michigan, 48824, USA

[d] Department of Environment and Geography, University of York, Heslington, York, YO10 5NG, UK

[e] Department of Earth, Atmospheric and Planetary Sciences, 550 Stadium Mall, Purdue University, West Lafayette, IN 47907, USA

Corresponding author: Cliff T. Johnston

Fax: +1-7654961716

E-mail: cliffjohnston@purdue.edu

Abstract

Polychlorinated dibenzo-p-dioxins and -furans (PCDD/PCDFs) are highly toxic organic pollutants in soils and sediments which persist over timescales that extend from decades to centuries. There is a growing need to develop effective technologies for remediating PCDD/Fs-contaminated soils and sediments to protect human and ecosystem health. The use of sorbent amendments to sequester PCDD/Fs has emerged as one promising technology. A synthesis method is described here to create a magnetic activated carbon composite (AC-Fe_3O_4) for dioxin removal and sampling that could be recovered from soils using magnetic separation. Six AC-Fe_3O_4 composites were evaluated (five granular ACs (GACs) and one fine-textured powder AC(PAC)) for their magnetization and ability to sequester dibenzo-p-dioxin (DD). Both GAC/PAC and GAC/PAC-Fe_3O_4 composites effectively removed DD from aqueous solution. The sorption affinity of DD for GAC-Fe_3O_4 was slightly reduced compared to GAC alone, which is attributed to the blocking of sorption sites. The magnetization of a GAC-Fe_3O_4 composite reached 5.38 emu/g based on SQUID results, allowing the adsorbent to be easily separated from aqueous solution using an external magnetic field. Similarly, a fine-textured PAC-Fe_3O_4 composite was synthesized with a magnetization of 9.3 emu/g.

Keywords: dibenzo-p-dioxin, granular activated carbon, Fe_3O_4, magnetic separation,

activated carbon-Fe_3O_4 composite

1. Introduction

Polychlorinated dibenzo-p-dioxins (PCDDs) are prototypical persistent organic pollutants (POPs) that are commonly found in soils and sediments. Due to their exceptionally low water solubilities, these highly toxic lipophilic substances are highly bio-accumulative (Guruge et al., 2005; Maier et al., 2016; Champoux et al., 2017). Exposure to PCDDs, even at trace concentrations (Denison et al., 1989; Eljarrat et al., 2002), can result in measurable toxic and carcinogenic effects in mammals (Huwe, 2002; McKay, 2002; Charnley and Doull, 2005). PCDDs occur both naturally and from anthropogenic activities which include forest fires, coal combustion, iron ore sintering, chlorine bleaching of pulp and paper, waste incineration, and as by-products of pesticide manufacturing and the chlor-alkali process (Fiedler, 1996; Everaert and Baeyens, 2002; Kulkarni et al., 2008; Zheng et al., 2008; Zhou et al., 2016; Prisciandaroa et al., 2017; Zhao et al., 2017). Owing to their lipophilicity, PCDD/Fs accumulate in surface soils, sediments and biota, including the fatty tissues of fish (WHO, 2010). In natural environments, they occur predominantly in the sorbed state associated with pyrogenic carbonaceous matter (PCM), amorphous organic matter, and clays (Ferrario et al., 2000; Fabietti et al., 2010). In fact, the significant role of PCM as a sorption domain has been well established (Cornelissen et al., 2005). As a group, PCDD/Fs are characterized by low aqueous solubilities and high octanol-water coefficients K_{ow} (Shiu et al., 1988; Kim et al.,

2002; Li et al., 2009). Consequently, their concentrations in natural waters are extremely low with concentration ranges of pg/L to fg/L (Charlestra et al., 2008; Cornelissen et al., 2008b; Louchouarn et al., 2018). PCDD/F-contaminated soils are found in ecosystems worldwide (Masunaga et al., 2001; Moon et al., 2008; Zheng et al., 2008), and have proven difficult and expensive to remediate. For example, the estimated cleanup cost of a *single* Superfund site along the Passaic River which is contaminated by PCDD/Fs has exceeded one billion US dollars.

Traditional site remediation has relied on removal of the contaminants via excavation or dredging followed by disposal in a hazardous waste landfill. Recently, sorbent amendments have gained attention as a means to lower or even eliminate bioavailability of soil/sediment-bound contaminants (Ghosh et al., 2011; Cornelissen et al., 2012; Hale et al., 2012; Cornelissen et al., 2016; Cho et al., 2017), and this has formed the basis of a new direction in management of sites contaminated with PCDD/Fs (Ghosh et al., 2011). Activated carbon (AC) materials (including granular activated carbon (GAC) and powdered activated carbon (PAC), has emerged as an effective sorbent amendment for this purpose (Cornelissen et al., 2012; Denyes et al., 2013; Gomez-Eyles et al., 2013; Balasubramani and Rifai, 2018).

The retrieval of the amendment with its sorbed contaminants after deployment has become a priority for a number of reasons. First, complete removal of contaminants, rather than just immobilization, is preferred by many environmental regulatory agencies (e.g.,

77 USEPA, 1997). Second, recovery of the sorbent amendment after its use as a passive sampler
78 can help determine mass transfer kinetics (Cornelissen et al., 2008a; Oen et al., 2011).
79 Adsorbent magnetization is an emerging remediation area where magnetic separation
80 simplifies isolation and regeneration (Mohan et al., 2014). Numerous studies have
81 demonstrated that activated carbon/Fe_3O_4 composites can be synthesized that maintain high
82 surface area and high sorption affinities for a growing list of contaminants that includes
83 organic dyes (Do et al., 2011), arsenic (Zhang et al., 2007, Zhang et al., 2010), heavy metals
84 (Han et al., 2015), pesticides and PAHs (Mohan et al., 2014). Our previous work showed
85 that magnetic Fe_3O_4 can be easily fabricated from the hydrothermal ferrite process and has
86 the potential to remove/recover toxic/precious elements from aqueous solutions (Tu et al.,
87 2012; Tu et al., 2013; Tu et al., 2015). To date, adsorbent magnetization has not been applied
88 to applications involving PCDD/Fs.

89 In our prior work, we provided the first evidence that bioavailability of TCDD sorbed to
90 two contrasting GACs and one PAC was eliminated in the mammalian (mouse) model. This
91 conclusion was based upon the use of two highly sensitive bioassays, hepatic induction of
92 cyp1A1 mRNA, an indirect measure of TCDD exposure, and immunoglobulin M antibody-
93 forming cell response, a direct measure of immune response (Boyd et al., 2017; Sallach et al.,
94 2019). Prior to this, reductions in bioavailability had only been established based on simpler
95 model organisms (e.g., worms) or passive samplers (Fagervold et al., 2010; Chai et al., 2011;

96 Chai et al., 2012). Although the ACs represented a wide range of particle size and pore size
97 distributions, they were equally effective in eliminating the bioavailability of TCDD, making
98 them viable candidates for remediation. In this study, we pursued an additional line of
99 investigation to determine if these same ACs could be functionalized using *in situ* synthesis
100 of Fe_3O_4 for subsequent magnetic retrieval (Indhu et al., 2015; Choi et al., 2016) without
101 compromising their affinity for dioxins.

102 AC-Fe_3O_4 composites were synthesized using the same GACs/PAC used in prior
103 bioavailability studies (Boyd et al., 2017; Sallach et al., 2019). The specific goals of the
104 current work were to (1) synthesize GAC/PAC-Fe_3O_4 composites using ACs shown to be
105 effective in eliminating TCDD bioavailability in mammals, with emphasis on gaining new
106 physicochemical insight into the interaction between GAC/PAC and Fe_3O_4, (2) characterize
107 the composites using a combination of X-ray diffraction (XRD), scanning electron
108 microscopy (SEM), N_2-BET and micropore analysis, and superconducting quantum
109 interference device (SQUID); and (3) evaluate sorption characteristics (kinetics and
110 equilibration) of GAC/PAC, Fe_3O_4, and the GAC/PAC-Fe_3O_4 composite for aqueous phase
111 dibenzo-p-dioxin (DD). The compound DD served as an isostructural conservative surrogate
112 for PCDD/Fs, which are important targets for sequestration using environmental geosorbents
113 due to their extreme recalcitrance in natural environments (Van Den Berg et al., 1998;
114 Sallach et al., 2019; Johnston et al., 2012).

2. Materials and methods

2.1. Chemicals and materials

All solutions were prepared with deionized water. Fe_3O_4 was synthesized from ferrous sulfate $FeSO_4$ (> 99.9%, Fisher Scientific, USA) and sodium hydroxide NaOH (99.5%, Fisher Scientific, USA). Dibenzo-p-dioxin (99% pure) was purchased from ChemService (West Chester, PA, USA) and was used as received. All the reagents are of analytical grade and used without further purification. Five GACs (DSRA, G60, FM-1, TOG-LF, and, F400) and one fine textured PAC (WPC) were purchased/obtained from USEPA, Sigma Aldrich, Cabot, Calgon Carbon Corp,. Selected physical properties of the six GACs/PAC are given in Table 1.

2.2. Synthesis procedure for magnetic AC-Fe_3O_4 composites

The magnetic GAC/PAC-Fe_3O_4 composite synthesis followed two synthesis procedures modified from our previously published method (Tu et al., 2013). Method A was performed using 0.01 M $FeSO_4$ at T=338 K, pH 10, and a reaction time of 2 h. Method B was carried out using 0.1 M $FeSO_4$ at T=298 K, pH 10, and the same 2 h reaction time. Briefly, one gram of GAC/PAC material was dried under vacuum at room temperature for 20 h using a vacuum oven (Model 280 A, Fisher Scientific, USA). Dried GAC/PAC was then immersed in 0.01 M (Method A) or 0.1 M (Method B) $FeSO_4$ solution (0.5 L) and mixed continuously at room temperature for 20 h. After mixing, the pH was adjusted to 10 by dropwise addition of 0.1 M

NaOH and then air was bubbled to the solution to initiate the reaction. The synthesis reactions were carried out at 338 K (Method A) or 298 K (Method B) for 2 h while maintaining the pH at 10. Finally, the resultant AC-Fe_3O_4 material was rinsed 5x with DI water to remove free Fe_3O_4, and successfully magnetized GAC/PAC-Fe_3O_4 composites was separated from the solution via magnet. The corresponding synthetic reaction of Fe_3O_4 can be described as Eq. 1 (Tu et al., 2013).

$$3\ Fe^{2+} + 6\ OH^- + 1/2\ O_2 \rightarrow Fe_3O_4 + 3\ H_2O \quad \text{.....(1)}$$

2.3. Characterization of AC-Fe_3O_4 composite

The crystal phases were determined by X-ray diffraction (XRD; X'Pert Pro, Philips, Netherlands) using graphite monochromatic cobalt radiation over the 2θ range 10-80°. The surface morphology and particle size were examined by scanning electron microscopy (SEM; Nova NanoSEM, Oxford instruments, UK). The saturation magnetization of the adsorbent was measured using a Superconducting Quantum Interference Device (SQUID magnetometer; MPMS-3, Quantum Design, USA) at 300 ±1 K. N_2 BET and micropore analysis was conducted using a Micromeritics 3Flex Multiport Chemi/Physi/Micropore Analyzer.

2.4. Measurement of adsorption isotherm

Batch adsorption experiments were conducted in duplicate using five initial aqueous DD concentrations (0.18, 0.3, 0.4, 0.6 and 0.8 mg/L) prepared by a serial dilution of 800 mg/L of

153 DD methanol stock solution. The amount of methanol in the aqueous solutions was 0.1%
154 which is considered to have minimal cosolvent effects. Aqueous solutions of DD were
155 sonicated for 60 min at room temperature in a water bath sonicator prior to mixing with the
156 GAC/PAC (Branson 120, Branson Ultrasonics, Danbury, CT, USA).

157 Two and half (2.5) mg of the adsorbent (GAC, PAC, GAC-Fe_3O_4, PAC-Fe_3O_4) was
158 placed in 30 mL Corex glass tubes (Kimble, Vineland, NJ, USA) with
159 polytetrafluoroethylene (PTFE)-lined screw caps, and mixed with a 30 mL aliquot of DD in
160 aqueous solutions (methanol 0.1 %). Control samples containing the initial aqueous DD
161 solutions 0.6 and 0.8 mg/L of DD solution without AC were prepared for calibration to
162 determine the losses of DD in the batch reactor. Measured values of DD in the control
163 samples ranged from 0.58 to 0.62 mg/L and 0.78 to 0.82 mg/L for the 0.6 and 0.8 mg/L DD
164 solutions, respectively. These results indicated that loss of DD to glassware can be ignored.

165 The suspensions were sonicated for 30 sec prior to shaking at a speed of 60 rpm in a rotary
166 shaker (Glas-Col, Terre Haute, IN, USA) at room temperature for 10-48 h to achieve the
167 apparent sorption equilibrium. The supernatant and adsorbent were separated by
168 centrifugation for GAC/PAC and by external magnetic field for GAC/PAC-Fe_3O_4
169 composites. An aliquot of 1.0 mL of supernatant and DD standards (0.0, 0.18, 0.3, 0.4, 0.6
170 and 0.8 mg/L) were transferred to HPLC vials. In order to prevent any sorption of DD by
171 HPLC vials, 0.5 mL of methanol (99.9%) was added to each vial prior to the addition of the

supernatant. HPLC vials containing supernatant and methanol were vortexed for 30 sec using a digital mini-vortexer (VWR, Radnor, PA, USA). Samples were then analyzed for DD concentrations by direct injection of 50 µL into a Thermo Scientific high-performance liquid chromatography (HPLC) system (Ultimate 3000) equipped with a UV detector and a 150× 4.60 mm 5 micron Luna 5 µm C8(2) 100 Å column (S/N 514816-4). Isocratic elution was performed using a mobile phase of 80% methanol: 20% water (v/v) with a flow rate of 1.0 mL/min and wavelength of 223 nm for detection.

The amount of DD sorbed (q_e, mg/kg) was calculated as the difference between the amount initially added and that remaining in the solution after equilibration (Eq. 2):

$$q_e = \frac{(C_o - C_e) \times V}{m_{ads}} \quad \text{.....(2)}$$

where C_o and C_e are DD concentration in liquid phase at time zero and after equilibration (mg/L), respectively; V is the solution volume used in DD adsorption (L); m_{ads} is GAC/PAC mass (kg).

2.5. Desorption

Following collection of the supernatant after equilibrium had been reached, the remaining supernatant was carefully decanted and the solid phase was re-suspended in a 30 mL solution of 25% and 99.9% methanol and water (v/v). Tubes were sonicated for 30 sec prior to shaking 24 h at 60 rpm to ensure equilibrium. Then, the supernatant and adsorbent were separated by either centrifugation (GAC/PAC) or external magnetic field (GAC/PAC-Fe_3O_4

composite). Approximately 1.5 mL aliquots of supernatant and standards of 0.18, 0.3, 0.4, 0.6 and 0.8 mg/L were transferred to HPLC vials for HPLC analysis. The amount of DD desorbed was calculated directly from the concentration of DD present in the supernatant following equation Eq. 3:

$$\text{Desorption efficiency} = \frac{C \times V}{X} \times 100\% \quad \text{.....(3)}$$

where C (mg/L) is the concentration of DD in the desorption solution, V (L) is the volume of the desorption solution, and X (g) is the amount of DD adsorbed.

3. Results and discussion

3.1. Adsorbent characterization in GAC

Six activated carbon materials consisting of five granular activated carbon (GAC) materials (F400, FM-1, G60, TOG-LF, and DSRA) and one fine textured powdered activated carbon powder (PAC) (WPC) were functionalized with Fe_3O_4. Selected physical properties of the six materials are given in Table 1. All but one of these GAC/PAC materials (DSRA) were used in recent TCDD bioavailability studies and were found to be highly effective in eliminating mammalian bioavailability of TCDD (Boyd et al., 2017; Sallach et al., 2019).

The activated carbon materials (Table 1) were functionalized using two different magnetite synthesis methods. Given their large specific surface areas and micropore (0-2 nm pores) volumes (Table 1), some magnetite synthesis was expected to occur in the micro- and

mesopores (2-50 nm pores) of the GAC/PAC, along with surface decoration of exterior surfaces of the GAC/PAC particles rendering the GAC/PAC-Fe_3O_4 composites magnetic. Fe_3O_4 synthesis Method A was performed at elevated temperature (338 K) using 0.01 M $FeSO_4$. The resulting magnetization of the PAC-Fe_3O_4 composite was successful with a value of 9.7 emu/g (Table 1). In contract, observed magnetization values measured at 300 K for the five GACs were weak with values of 0.61 (DSRA), 0.54 (FM-1), 0.49 (TOG-LF), 0.46 (G60) and 0.35 (F-400) emu/g (Table 1). For comparison, the magnetization of Fe_3O_4 synthesized using Synthesis Method A without GAC/PAC was 71.9 emu/g. Weak magnetization values in the ranged of 0.35-0.61 emu/g were not sufficient to allow rapid magnetic separation.

Because the magnetization values resulting from synthesis Method A for the granular activated carbon samples were weak (0.35-0.61 emu/g), the Fe_3O_4 synthesis procedure was modified using synthesis Method B, which utilized a higher concentration of $FeSO_4$ (0.1 M) and a lower temperature of 298 K. The granular activated carbon sample DSRA was selected because it showed the highest level of magnetization among the five GAC materials evaluated using Method A (Table 1). Synthesis Method B resulted in a DSRA-Fe_3O_4 composite with a significantly improved magnetization value of 5.38 emu/g (Table 1). No residual magnetism was detected in either of the GAC(DSRA)-Fe_3O_4 (Synthesis Method B) or PAC(WPC)/Fe_3O_4 (Synthesis Method A) composites indicating that these two materials are superparamagnetic (Table 1). For simplicity, the GAC(DSRA)-Fe_3O_4 complex (using

229 Synthesis Method B) will be referred to as GAC-Fe_3O_4(B) and the PAC(WPC)-Fe_3O_4

230 complex (using Synthesis Method A) will be referred to as PAC-Fe_3O_4(A), where (A) and

231 (B) refer to Synthesis Methods A and B, respectively.

232 The GAC-Fe_3O_4(B) composite in aqueous suspension was efficiently recovered by

233 applying an external magnetic field. The complete (~100%) separation of the GAC-Fe_3O_4(B)

234 composite from solution using a magnet was achieved within only 20 seconds (Supplemental

235 Information Fig. S1). When the external magnetic field was removed, the GAC-Fe_3O_4(B)

236 composite could be readily dispersed again in water by physical shaking.

237 The XRD patterns of the GAC-Fe_3O_4(B) and PAC-Fe_3O_4(A) composites are shown in

238 Fig. 2. The observed diffraction peaks at d-spacings of 4.846, 2.968, 2.531, 2.423, 2.099,

239 1.713, 1.615, and 1.484 Å matched the XRD reflections of Fe_3O_4 (JCPDS file number 04-

240 007-9093). No other peaks were detected in the XRD pattern of the GAC-Fe_3O_4(B)

241 confirming that the only crystalline phase present is Fe_3O_4 nanoparticles in the GAC-

242 Fe_3O_4(B) composite. In addition to the Fe_3O_4 peaks, the PAC-Fe_3O_4(A) composite had small

243 peaks at 24.2, 31.0 and 58.5 °2θ.

244 Further characterization of the GAC and the GAC-Fe_3O_4(B) composite was provided by

245 SEM imaging of the two materials at different levels of magnification (Figs. 3a-3f). The

246 average bulk size of the GAC was ~1 mm with <5% passing through a 40 US Mesh sieve

247 (420 μm) (Fig. 3a); 'large' pores were observed ranging in size from several μm to >10 μm

248 (Figs. 3b and 3c). The synthesized Fe_3O_4 particles were observed to be spherical, and their
249 primary particle size ranged between 20 and 120 nm (Fig. 3d). From the SEM images it is
250 evident that the synthesized Fe_3O_4 nanoparticles were randomly distributed on the surfaces
251 and pores of the GAC particles (Fig. 3f).

252 3.2 N_2 BET and Textural Analysis

253 N_2 BET and micro-textural analysis of the activated carbon materials prior to magnetite
254 synthesis are presented in Table 1. The supplier of the activated carbon, feedstock, along with
255 N_2 BET surface area and micropore analysis are presented in Table 1. The five granular
256 activated carbon samples ranged in percentage micropore (0-2 nm) volume from 29 to 82%
257 of the total micropore and mesopore (2-50 nm) volume. The fine textured WPC powder had
258 very little mesoporosity with 91% of its pore volume in the micropore range. Of the six
259 samples, five were used in prior toxicology studies to assess TCDD bioavailability (Boyd et
260 al., 2017; Sallach et al., 2019). Although these ACs represented a wide range of particle size
261 and pore size distributions, they were equally effective in eliminating the bioavailability of
262 TCDD, making them viable candidates for remediation. After Fe_3O_4 synthesis, the specific
263 surface area of the GAC(DSRA)-Fe_3O_4 composite decreased from 822 to 633 m^2/g along
264 with a modest reduction in micropore volume (0.388 to 0.262 g/cc) indicative of some partial
265 pore blocking by the magnetite particles (Table 1).

3.3. Batch equilibrium sorption and kinetics

Batch sorption isotherms of dibenzo-p-dioxin (DD) to GAC and GAC-Fe_3O_4(B) are shown in Fig. 4. Both GAC and GAC-Fe_3O_4 composite showed a high affinity for aqueous phase DD at low equilibrium concentrations (<0.005 mg/L) up to a sorbed concentration about of about 4000 mg/kg. At higher equilibrium concentrations (0.005-0.12 mg/L), sorption isotherms showed some nonlinear behavior exhibiting high affinity at low equilibrium concentration followed by an "S-shaped" response (Giles and Smith, 1974). The GAC-Fe_3O_4(B) isotherm is shifted to higher equilibrium concentrations (i.e., lower affinity) compared the GAC, however, both materials sorbed > 8000 mg/kg. These results could be explained by sorption processes involving easily accessible external sites and less accessible pores. Since Fe_3O_4 demonstrated no sorption affinity for DD, its presence within the GAC composite likely blocked some sorption sites or access to certain pores manifesting a slight decrease in DD affinity.

The kinetics of DD sorption by GAC and GAC-Fe_3O_4 composite were evaluated over a period of 40 h using the batch equilibration method (described above) with initial aqueous phase DD concentrations of 0.18, 0.4, and 0.8 mg/L (Fig. 5). Sorption kinetics of DD can be separated into two phases. Initially, within the first 10 h, both GAC and GAC-Fe_3O_4 demonstrated comparatively rapid uptake of DD for all three initial concentrations. This was followed by a slower phase (>50 h) to reach apparent equilibrium.

For the lower and intermediate initial DD concentrations of 0.18 and 0.4 mg/L, DD uptake from aqueous solution by GAC was rapid and nearly complete within the first 10 h; the percent DD removal approached 100 percent (Fig 5c-f). However, at the higher initial DD concentration of 0.8 mg/L, there is a more gradual approach to apparent equilibrium over time (Fig. 5a-b). For the initial concentrations of 0.18 and 0.4 mg/L, DD adsorption by GAC was essentially complete by 10 h, and the total uptake of DD from aqueous solution approached 100 percent. For the initial concentration of 0.8 mg/L the data indicate that equilibrium had not been achieved after 50 h for GAC-Fe_3O_4.

For this system, it is assumed that sorption kinetics are controlled surface adsorption with associated resistance to film diffusion followed by an emerging contribution to DD sorption via intraparticle diffusion. Pseudo-second order kinetic models are commonly used to describe sorption kinetics for these types of interactions (Ho and, McKay, 1999; Amarasinghe and Williams, 2007). The pseudo-second order kinetic model was able to fit the experimental data well (see Table 2). The pseudo-second order model results are plotted on the kinetics data shown in Fig. 5.

The correlation coefficients (R^2) and kinetic parameters derived from the pseudo-second order models are summarized in Table 2. These results suggest that the rate-limiting step may be some type of site-specific mechanism involving direct interaction between the sorbent and sorbate (Amarasinghe and Williams, 2007). The kinetic rate constant (k_2) from the pseudo-

304 second order model decreased with increasing initial DD concentrations (Table 1), indicating
305 that the DD adsorption rates are faster at lower concentrations. In other words, the time
306 required to reach equilibrium increased as the initial DD concentration increased. This is
307 likely due to competition for active surface sites and pores of the sorbent which is greater at a
308 higher DD concentration.

309 3.4 Desorption of DD

310 Desorption of DD into solutions of either 25% or 99.9% methanol and water (v/v)
311 desorption solutions were used to evaluate the reversibility of DD sequestration by GAC and
312 the GAC-Fe_3O_4 composite. Desorption of DD from GAC and GAC-Fe_3O_4 in 99.9% methanol
313 was 19% and 14.3% (after 20 h), respectively, and 11.2% and 12.4% for 25%
314 methanol/water, respectively. These results agree with our prior study that showed 22-27%
315 of TCDD bound to three of the activated carbons samples used in the present study could be
316 desorbed after 64 hours of Soxhlet extraction using toluene (Sallach et et., 2019).
317 Magnetizing GAC with Fe_3O_4 had little to no effect on the propensity of DD to desorb. That
318 the fraction of released DD was less than 20% even for 99.9% methanol clearly indicated the
319 strong affinity between DD and GAC; once sorbed DD appears to be largely irreversibly-
320 sequestered within the pore structure of GAC. The resistance to desorption, even into
321 methanol, is consistent with our prior observation that sequestration of 2,3,7,8-TCDD by AC
322 eliminated its mammalian bioavailability (Boyd et al., 2017; Stedtfeld et al., 2017).

3.5 Sorption removal comparison of fine-textured AC-Fe_3O_4 to GAC-Fe_3O_4

The uptake of DD by GAC, GAC-DSR-Fe_3O_4(B), PAC and PAC-Fe_3O_4(A) as a function of time are shown in Fig. 6. As expected, uptake of DD by the fine-textured AC (WPC) was rapid and nearly stoichiometric. More than 90% of the WPC has a particle size of < 45 μm (Sallach et al., 2019). In contrast, sorption kinetics for DD uptake by the coarse-textured GAC and GAC-Fe_3O_4(B) were considerably slower. Although the surface area of the PAC, GAC and their Fe_3O_4 derivatives are comparable, most of the surface area in GAC can only be accessed through intraparticle diffusion, resulting in slower sorption kinetics (Figs. 5-6).

4. Discussion

The activated carbon materials, including GAC and PAC, used here to form the magnetic variants were also used in our prior bioavailability studies (Boyd et al., 2017; Stedtfeld et al., 2017; Sallach et al., 2019), along with natural geosorbents including clay minerals and silica (Boyd et al., 2011; Kaplan et al., 2011; Chai et al., 2016). Among these, only GAC and PAC eliminated the bioavailability of sorbed TCDD to a mammalian (mouse) model. Mammalian bioavailability was evaluated in our prior work using two highly sensitive bioassays, hepatic induction of cyp1A1 mRNA, an indirect measure of TCDD exposure, and immunoglobulin M antibody-forming cell response, a direct measure of immune response (Boyd et al., 2017; Sallach et al., 2019). In contrast to the complete elimination of TCDD bioavailability achieved via sequestration by GAC/PAC, TCDD bound to clay minerals and

342 silica was found to be 100% bioavailable. The lack of mammalian bioavailability of TCDD
343 bound to GAC/PACs was consistent with a related study showing contaminant bioavailability
344 to lower organisms was significantly decreased in the presence of AC (Chai et al., 2012). In
345 addition, attempts to extract sorbed TCDD from ACs using Soxhlet extraction revealed that
346 only a minor fraction of the total TCDD present could be recovered (Sallach et al., 2019).
347 From an applied perspective, these laboratory results are now leading to the use of GAC/PAC
348 sorbent amendments in large-scale remediation efforts for impacted soils, sediments and
349 water bodies (Samuelsson et al., 2017; Payne et al., 2019; Cornelissen et al., 2016;
350 Beckingham et al., 2011). Given our earlier results showing elimination of mammalian
351 TCDD bioavailability, creating magnetic GAC/PAC composites that could be used as a
352 retrievable form of GAC/PAC sorbent amendments was attempted. The ability to retrieve
353 magnetized GAC/PAC would enhance their utility as passive samplers in field settings and in
354 ongoing laboratory studies. For example, our earlier mammalian studies would have
355 benefited from using a magnetic AC to determine the amount TCDD in fecal pellets from
356 mice that were dosed with TCDD–AC (Boyd et al., 2017; Stedfeldt et al., 2017; Sallach et al.,
357 2018). Likewise, the ability to ultimately retrieve (magnetized) GAC/PAC sorbent
358 amendments used to remediate areas with especially high levels of contamination would
359 provide both an immediate benefit, i.e., bioavailability reduction, and make contaminant
360 removal possible in the longer term.

361 The synthesis procedure using a lower concentration of $FeSO_4$ (0.01 M) at an elevated
362 temperature (338 K), Synthesis Method A, was successful in synthesizing a magnetic PAC-
363 Fe_3O_4 composite (PAC-Fe_3O_4(A)). In the case of the PAC, magnetization most likely
364 occurs on the external surfaces of fine-textured AC and this could be accomplished using the
365 lower concentration of $FeSO_4$. However, Method A only produced weak magnetization
366 values for the GAC-Fe_3O_4 composites. One could argue that this procedure was not able to
367 synthesize Fe_3O_4 particles within the coarse textured GACs. The procedure was modified
368 using a higher concentration of $FeSO_4$ (0.1 M) and lower temperature that resulted in a
369 sufficiently magnetic GAC-Fe_3O_4(B) composite.

370 Both the GAC-Fe_3O_4(B) and PAC-Fe_3O_4(A) composites revealed the presence of Fe_3O_4
371 based on X-ray diffraction analysis (Fig. 2) and it is possible that careful XRD studies could
372 be used as a surrogate for the more difficult to obtain SQUID magnetization results. N_2 BET
373 surface area and textural analysis showed that both the GAC and PAC materials were
374 characterized by high N_2-surface area (802-822 m^2/g). The specific surface area of the
375 GAC-Fe_3O_4(B) composite showed a modest reduction in both surface area (822 to 633 m^2/g)
376 and micropore volume (0.38 g/cc to 0.26 g/cc) compared to the starting GAC (Table 1).
377 The batch sorption isotherms of dibenzo-p-dioxin (DD) on the GAC and GAC-Fe_3O_4(B)
378 composites showed that sorption affinity of DD was slightly reduced due to the presence of
379 magnetite particles (GAC-Fe_3O_4(B)) compared GAC. The decrease in surface area and DD

sorption is interpreted as some blocking of pore throats. Overall, the sorption isotherms for both GAC and GAC-Fe_3O_4(B) showed some sorption nonlinearity, consistent with a range of sorption sites of varying accessibility.

The sorption kinetics of DD uptake by GAC, GAC-Fe_3O_4(B), PAC and PAC-Fe_3O_4(A) were strongly dependent on particle size. Uptake of DD by the fine textured PAC and PAC-Fe_3O_4(A) composite was rapid and complete within 10 hours. In contrast, sorption uptake was much slower for GAC and the GAC-Fe_3O_4(B) composite (Fig. 4 and 5) owing to the larger particle size. Sorption equilibria had not been reached for the GAC-Fe_3O_4(B) composite after 40 h. These results are consistent with prior work showing the influence of particle size on sorption kinetics of hydrophobic organic solutes on activated carbon and biochars (Ahn et al., 2005; Kang et al., 2018). As shown, the rate of DD uptake by the fine textured AC and AC-Fe_3O_4(A) is rapid with showing 97% removal of DD from aqueous solution after one hour. The larger sized GAC, with particle diameters ~ 1 mm (5% < 420 μm), showed much slower uptake (Fig. 6a) and is attributed to the longer diffusion pathways to binding sites and pore structures in GAC.

We demonstrated that both a GAC and a PAC could be magnetized and, more importantly, the GAC-Fe_3O_4(B) and PAC-Fe_3O_4(A) composites maintained high sorption affinity for dioxin. Particle size was a dominant factor in controlling sorption kinetics, with the fine-textured PAC showing nearly complete uptake of dioxin within 1 hour compared to

considerably slower uptake by the coarse texture GAC. These differences could be significant in animal dosing studies but less significant for materials deployed as passive samplers over periods of months to years. Finally, these results could prove useful in the design of large-scale recoverable geosorbents manufactured for contaminant removal.

Acknowledgments

Research reported in this paper was supported by the National Institute of Environmental Health Sciences and Shanghai Natural Science Foundation under Award Number P42ES004911and 20ZR1441100, respectively. The content is solely the responsibility of the authors and does not necessarily represent the official views of the National Institutes of Health. The authors appreciate Dr. Timothy Henderson and Dr. Neil R. Dilley (Birck Nanotechnology Center) for their support with SEM and SQUID analysis.

References

Ahn, S., Werner, D., Karapanagioti, H.K., McGlothlin, D.R., Zare, R.N., Luthy, R.G., 2005. Phenanthrene and pyrene sorption and intraparticle diffusion in polyoxymethylene, coke, and activated carbon. Environ. Sci. Technol. 39, (17), 6516-6526.

Amarasinghe, B.M.W.P.K., Williams, R.A., 2007. Tea waste as a low cost adsorbent for Cu and Pb removal from wastewater. Chem. Eng. J. 132, 299-309.

Balasubramani, A., Rifai, H.S., 2018. Efficacy of carbon-based materials for remediating

418 polychlorinated biphenyls (PCBs) in sediment. Sci. Total Environ. 644, 398-405.
419 Beckingham, B., Ghosh, U., 2011. Field-Scale Reduction of PCB Bioavailability with
420 Activated Carbon Amendment to River Sediments. Environmental Science & Technology
421 45, 10567-10574.
422 Boyd, S.A., Johnston, C.T., Pinnavaia, T.J., Kaminski, N.E., Teppen, B.J., Li, H., Khan, B.,
423 Crawford, R.B., Kovalova, N., Kim, S.S., Shao, H., Gu, C., Kaplan, B.L.F., 2011.
424 Suppression of humoral immune responses by 2,3,7,8-tetrachlorodibenzo-p-dioxin
425 intercalated in smectite clay. Environ. Toxicol. Chem. 30, (12), 2748-2755.
426 Boyd, S.A., Sallach, J.B., Zhang, Y., Crawford, R., Li, H., Johnston, C.T., Teppen, B.J.,
427 Kaminski, N.E., 2017. Sequestration of 2,3,7,8-tetrachlorodibenzo-p-dioxin by activated
428 carbon eliminates bioavailability and the suppression of immune function in mice.
429 Environ. Toxicol. Chem. 36, 2671-2678.
430 Champoux, L., Rail, J.F., Lavoie, R.A., 2017. Polychlorinated dibenzo-p-dioxins,
431 dibenzofurans, and flame retardants in northern gannet (Morus bassanus) eggs from
432 Bonaventure Island, Gulf of St. Lawrence, 1994-2014. Environ. Pollut. 222, 600-608.
433 Charlestra, L., Courtemanch, D.L., Amirbahman, A., Patterson, H., 2008. Semipermeable
434 membrane device (SPMD) for monitoring PCDD and PCDF levels from a paper mill
435 effluent in the Androscoggin River, Maine, USA. Chemosphere 72, 1171-1180.
436 Chai, B.L., Tsoi, T.V., Iwai, S., Liu, C., Fish, J.A., Gu, C., Johnson, T.A., Zylstra, G., Teppen,

437 B.J., Li, H., Hashsham, S.A., Boyd, S.A., Cole, J.R., Tiedje, J.M., 2016. Sphingomonas
438 wittichii strain RW1 genome-wide gene expression shifts in response to dioxins and clay.
439 Plos One 11, (6), 14.
440 Chai, Y.Z., Currie, R.J., Davis, J.W., Wilken, M., Martin, G.D., Fishman, V.N., Ghosh, U.,
441 2012. Effectiveness of activated carbon and biochar in reducing the availability of
442 polychlorinated dibenzo-p-dioxins/dibenzofurans in soils. Environ. Sci. Technol. 46 (2),
443 1035-1043.
444 Chai, Y.Z., Davis, J.W., Wilken, M., Martin, G.D., Mowery, D.M., Ghosh, U., 2011. Role of
445 black carbon in the distribution of polychlorinated dibenzo-p-dioxins/dibenzofurans in
446 aged field-contaminated soils. Chemosphere 82 (5), 639-647.
447 Charnley, G., Doull, J., 2005. Human exposure to dioxins from food, 1999-2002. Food Chem.
448 Toxicol. 43, 671-679.
449 Cho, D.W., Yoon, K., Kwon, E.E., Biswas, J.K., Song, H., 2017. Fabrication of magnetic
450 biochar as a treatment medium for As(V) via pyrolysis of $FeCl_3$-pretreated spent coffee
451 ground. Environ. Pollut. 229, 942-949.
452 Choi, Y.J., Wu, Y.W., Sani, B., Luthy, R.G., Werner, D., Kim, E., 2016. Performance of
453 retrievable activated carbons to treat sediment contaminated with polycyclic aromatic
454 hydrocarbons. J. Hazard. Mater. 320, 359-367.
455 Cornelissen, G., Amstaetter, K., Hauge, A., Schaanning, M., Beylich, B., Gunnarsson, J.S.,

456 Breedveld, G.D., Oen, A.M.P., Eek, E., 2012. Large-scale field study on thin-layer
457 capping of marine PCDD/F-contaminated sediments in Grenlandfjords, Norway:
458 physicochemical effects. Environ. Sci. Technol. 46, 12030-12037.
459 Cornelissen, G., Arp, H.P.H., Pettersen, A., Hauge, A., Breedveld, G.D., 2008a. Assessing
460 PAH and PCB emissions from the relocation of harbour sediments using equilibrium
461 passive samplers. Chemosphere 72, 1581-1587.
462 Cornelissen, G., Gustafsson, O., Bucheli, T.D., Jonker, M.T.O., Koelmans, A.A., Van Noort,
463 P.C.M., 2005. Extensive sorption of organic compounds to black carbon, coal, and
464 kerogen in sediments and soils: Mechanisms and consequences for distribution,
465 bioaccumulation, and biodegradation. Environ. Sci. Technol. 39, 6881-6895.
466 Cornelissen, G., Schaanning, M., Gunnarsson, J.S., Eek, E., 2016. A large-scale field trial of
467 thin-layer capping of PCDD/F-contaminated sediments: sediment-to-water fluxes up to 5
468 years post-amendment. Integr. Environ. Assess. Manag. 12, 216-221.
469 Cornelissen, G., Wiberg, K., Broman, D., Arp, H.P.H., Persson, Y., Sundqvist, K., Jonsson, P.,
470 2008b. Freely dissolved concentrations and sediment-water activity ratios of PCDD/Fs
471 and PCBs in the open Baltic Sea. Environ. Sci. Technol. 42, 8733-8739.
472 Denison, M.S., Fisher, J.M., Whitlock Jr, J.P., 1989. Protein-DNA interactions at recognition
473 sites for the dioxin-Ah receptor complex. J. Biol. Chem. 264, 16478-16482.
474 Denyes, M.J., Rutter, A., Zeeb, B.A., 2013. In situ application of activated carbon and biochar

475 to PCB-contaminated soil and the effects of mixing regime. Environ. Pollut. 182, 201-208.
476 Do, M.H., Phan, N.H., Nguyen, T.D., Thi, T.S.P., Nguyen, V.K., Thi, T.T.V., Thi, K.P.N.,
477 2011. Activated carbon/Fe_3O_4 nanoparticle composite: Fabrication, methyl orange
478 removal and regeneration by hydrogen peroxide. Chemosphere 85, 1269-1276.
479 Eljarrat, E., Monjonell, A., Caixach, J., Rivera, J., 2002. Toxic potency of polychlorinated
480 dibenzo-p-dioxins, polychlorinated dibenzofurans, and polychlorinated biphenyls in food
481 samples from Catalonia (Spain). J. Agric. Food Chem. 50, 1161-1167.
482 Everaert, K., Baeyens, J., 2002. The formation and emission of dioxins in large scale thermal
483 processes. Chemosphere 46, 439-448.
484 Fabietti, G., Biasioli, M., Barberis, R., Ajmone-Marsan, F., 2010. Soil contamination by
485 organic and inorganic pollutants at the regional scale: The case of piedmont, Italy. J. Soil.
486 Sediment. 10, 290-300.
487 Fagervold, S.K., Chai, Y.Z., Davis, J.W., Wilken, M., Cornelissen, G., Ghosh, U., 2010.
488 Bioaccumulation of polychlorinated dibenzo-p-dioxins/dibenzofurans in E. fetida from
489 floodplain soils and the effect of activated carbon amendment. Environ. Sci. Technol. 44
490 (14), 5546-5552.
491 Ferrario, J.B., Byrne, C.J., Cleverly, D.H., 2000. 2,3,7,8-dibenzo-p-dioxins in mined clay
492 products from the united states: Evidence for possible natural origin. Environ. Sci.
493 Technol. 34, 4524-4532.

494 Fiedler, H., 1996. Sources of PCDD/PCDF and impact on the environment. Chemosphere 32,
495 55-64.
496 Ghosh, U., Luthy, R.G., Cornelissen, G., Werner, D., Menzie, C.A., 2011. In situ sorbent
497 amendments: A new direction in contaminated sediment management. Environ. Sci.
498 Technol. 45, 1163-1168.
499 Giles, C.H., Smith, D., Huitson, A., 1974. A general treatment and classification of the solute
500 adsorption isotherm. I. Theoretical. Journal of Colloid and Interface Science 47, 755-765.
501 Gomez-Eyles, J.L., Yupangui, C., Beckingham, B., Riedel, G., Gilmour, C., Ghosh, U., 2013.
502 Evaluation of biochars and activated carbons for in-situ remediation of sediments
503 impacted with organics, mercury, and methylmercury. Environ. Sci. Technol. 47, 13721-
504 13729.
505 Guruge, K.S., Seike, N., Yamanaka, N., Miyazaki, S., 2005. Polychlorinated dibenzo-p-dioxins,
506 -dibenzofurans, and biphenyls in domestic animal food stuff and their fat. Chemosphere
507 58, 883-889.
508 Hale, S.E., Elmquist, M., Brandli, R., Hartnik, T., Jakob, L., Henriksen, T., Werner, D.,
509 Cornelissen, G., 2012. Activated carbon amendment to sequester PAHs in contaminated
510 soil: A lysimeter field trial. Chemosphere 87, 177-184.
511 Han, Z.T., Sani, B., Mrozik, W., Obst, M., Beckingham, B., Karapanagioti, H.K. Werner, D.,
512 2015. Magnetite impregnation effects on the sorbent properties of activated carbons and

513 biochars. Water Res. 70, 394-403.

514 Ho, Y.S., McKay, G., 1999. Pseudo-second order model for sorption processes. Process
515 Biochem. 34, 451-465.

516 Huwe, J.K., 2002. Dioxins in food: a modern agricultural perspective. J. Agric. Food. Chem.
517 50, 1739-1750.

518 Indhu, Z.T., Sani, B., Akkanen, J., Abel, S., Nybom, I., Karapanagioti, H.K., Werner, D., 2015.
519 A critical evaluation of magnetic activated carbon's potential for the remediation of
520 sediment impacted by polycyclic aromatic hydrocarbons. J. Hazard. Mater. 286, 41-47.

521 Johnston, C.T., Khan, B., Barth, E.F., Chattopadhyay, S., Boyd, S.A., 2012. Nature of the
522 interlayer environment in an organoclay optimized for the sequestration of dibenzo-p-
523 dioxin. Environ. Sci. Technol. 46, 9584-9591.

524 Kang, S., Jung, J., Choe, J.K., Ok, Y.S., Choi, Y., 2018. Effect of biochar particle size on
525 hydrophobic organic compound sorption kinetics: Applicability of using representative
526 size. Sci. Total Environ. 619, 410-418.

527 Kaplan, B.L.F., Crawford, R.B., Kovalova, N., Arencibia, A., Kim, S.S., Pinnavaia, T.J., Boyd,
528 S.A., Teppen, B.J., Kaminski, N.E., 2011. TCDD adsorbed on silica as a model for TCDD
529 contaminated soils: Evidence for suppression of humoral immunity in mice. Toxicology
530 282, (3), 82-87.

531 Kim, H.K., Masaki, H., Matsumur, T., Kamei, T., Magara, Y., 2002. Removal efficiency and

532 homologue patterns of dioxins in drinking water treatment. Water Res. 36, 4861-4869.
533 Kulkarni, P.S., Crespo, J.G., Afonso, C.A.M., 2008. Dioxins sources and current remediation
534 technologies-a review. Environ. Int. 34, 139-153.
535 Li, X.M., Peng, P.A., Zhang, S.K., Man, R., Sheng, G.Y., Fu, J.M., 2009. Removal of
536 polychlorinated dibenzo-p-dioxins and polychlorinated dibenzofurans by three coagulants
537 in simulated coagulation processes for drinking water treatment. J. Hazard. Mater. 162,
538 180-185.
539 Louchouarn, P., Seward, S.M., Cornelissen, G., Arp, H.P.H., Yeager, K.M., Brinkmeyer, R.,
540 Santschi, P.H., 2018. Limited mobility of dioxins near San Jacinto super fund site (waste
541 pit) in the Houston Ship Channel, Texas due to strong sediment sorption. Environ. Pollut.
542 238, 988-998.
543 Maier, D., Benisek, M., Blaha, L., Dondero, F., Giesy, J.P., Köhler, H.R., Richter, D., Scheurer,
544 M., Triebskorn, R., 2016. Reduction of dioxin-like toxicity in effluents by additional
545 wastewater treatment and related effects in fish. Ecotoxicol. Environ. Saf. 132, 47-58.
546 Masunaga, S., Yao, Y., Ogura, I., Nakai, S., Kanal, Y., Yamamuro, M., Nakanishi, J., 2001.
547 Identifying sources and mass balance of dioxin pollution in Lake Shinji Basin, Japan.
548 Environ. Sci. Technol. 35, 1967-1973.
549 McKay, G., 2002. Dioxin characterisation, formation and minimisation during municipal solid
550 waste (MSW) incineration: review. Chem. Eng. J. 86, 343-368.

551 Mohan, D., Sarswat, A., Ok, Y.S., Pittman, C.U., 2014. Organic and inorganic contaminants
552 removal from water with biochar, a renewable, low cost and sustainable adsorbent - A
553 critical review. Bioresource Technol. 160, 191-202.
554 Moon, H.B., Yoon, S.P., Jung, R.H., Choi, M., 2008. Wastewater treatment plants (WWTPs)
555 as a source of sediment contamination by toxic organic pollutants and fecal sterols in a
556 semienclosed bay in Korea. Chemosphere 73, 880-889.
557 Oen, A.M.P., Janssen, E.M.L., Cornelissen, G., Breedveld, G.D., Eek, E., Luthy, R.G., 2011.
558 In situ measurement of PCB pore water concentration profiles in activated carbon-
559 amended sediment using passive samplers. Environ. Sci. Technol. 45, 4053-4059.
560 Payne, R.B., Ghosh, U., May, H.D., Marshall, C.W., Sowers, K.R., 2019. A Pilot-Scale Field
561 Study: In Situ Treatment of PCB-Impacted Sediments with Bioamended Activated
562 Carbon. Environmental Science & Technology 53, 2626-2634.
563 Prisciandaroa, M., Piemonteb, V., di Celsoc, G.M., Ronconid, S., Capocelli, M., 2017.
564 Thermodynamic features of dioxins' adsorption. J. Hazard. Mater. 324, 645-652.
565 Sallach, J.B., Crawford, R., Li, H., Johnston, C.T., Teppen, B.J., Kaminski, N.E., Boyd, S.A.,
566 2019. Activated carbons of varying pore structure eliminate the bioavailability of 2,3,7,8-
567 tetrachlorodibenzo-p-dioxin to a mammalian (mouse) model. Sci. Total Environ. 650,
568 2231-2238.
569 Samuelsson, G.S., Raymond, C., Agrenius, S., Schaanning, M., Cornelissen, G., Gunnarsson,

570 J.S., 2017. Response of marine benthic fauna to thin-layer capping with activated carbon
571 in a large-scale field experiment in the Grenland fjords, Norway. Environmental Science
572 and Pollution Research 24, 14218-14233.
573 Shiu, W.Y., Doucette, W., Gobas, F.A.P.C., Andren, A., Mackay, D., 1988. Physical-chemical
574 properties of chlorinated dibenzo-p-dioxins. Environ. Sci. Technol. 22, 651-658.
575 Stedtfeld, R.D., Sallach, J.B., Crawford, R.B., Stedtfeld, T.M., Williams, M.R., Waseem, H.,
576 Johnston, C.T., Li, H., Teppen, B.J., Kaminski, N.E., Boyd, S.A., Tiedje, J.M., Hashsham,
577 S.A., 2017. TCDD administered on activated carbon eliminates bioavailability and
578 subsequent shifts to a key murine gut commensal. Appl. Microbiol. Biotechnol. 101,
579 7409-7415.
580 Tu, Y.J., Chang, C.K., You, C.F., Wang, S.L., 2012. Treatment of complex heavy metal
581 wastewater using a multi-staged ferrite process. J. Hazard. Mater. 209-210, 379-384.
582 Tu, Y.J., Lo, S.C., You, C.F., 2015. Selective and fast recovery of neodymium from seawater
583 by magnetic iron oxide Fe_3O_4. Chem. Eng. J. 262, 966-972.
584 Tu, Y.J., You, C.F., Chang, C.K., Wang, S.L., 2013. XANES evidence of arsenate removal
585 from water with magnetic ferrite. J. Environ. Manage. 120, 114-119.
586 USEPA, 1997. Rules of thumb for Superfund remedy selection; EPA 540-R-97-013, OSWER
587 9355.0-69, PB97-963301; U.S. Environmental Protection Agency: Washington, DC.
588 Van den Berg, M., Birnbaum, L., Bosveld, A.T.C., Brunstrom, B., Cook, P., Feeley, M., Giesy,

589 J.P., Hanberg, A., Hasegawa, R., Kennedy, S.W., Kubiak, T., Larsen, J.C., van Leeuwen,
590 F.X.R., Liem, A.K.D., Nolt, C., Peterson, R.E., Poellinger, L., Safe, S., Schrenk, D., Tillitt,
591 D., Tysklind, M., Younes, M., Waern, F., Zacharewski, T., 1998. Toxic equivalency
592 factors (TEFs) for PCBs, PCDDs, PCDFs for humans and wildlife. Environmental Health
593 Perspectives 106, 775-792.
594 WHO, 2010. Exposure to dioxins and dioxin-like substances: a major public health concern.
595 http://www.who.int/ipcs/features/dioxins.pdf.
596 Zhang, Q.L., Lin, Y.C., Chen, X., Gao, N.Y., 2007. A method for preparing ferric activated
597 carbon composites adsorbents to remove arsenic from drinking water. J. Hazard. Mater.
598 148, 671-678.
599 Zhang, S.J., Li, X.Y., Chen, J.P., 2010. Preparation and evaluation of a magnetite-doped
600 activated carbon fiber for enhanced arsenic removal. Carbon 48, 60-67.
601 Zhao, Y.Y., Zhan, J.Y., Liu, G.R., Zheng, M.H., Jin, R., Yang, L.L., Hao, L.W., Wu, X.L.,
602 Zhang, X., Wang, P., 2017. Evaluation of dioxins and dioxin-like compounds from a
603 cement plant using carbide slag from chlor-alkali industry as the major raw material. J.
604 Hazard. Mater. 330, 135-141.
605 Zheng, G.J., Leung, A., Jiao, L.P., 2008. Polychlorinated dibenzo-p-dioxins and diben-
606 zofurans pollution in China: sources, environmental levels and potential human health
607 impacts. Environ. Int. 34, 1050-1061.

608 Zhou, X.J., Buekens, A., Li, X.D., Ni, M.J., Cen, K.F., 2016. Adsorption of polychlorinated
609 dibenzo-p-dioxins/dibenzofurans on activated carbon from hexane. Chemosphere 144,
610 1264-1269.

611

612

613

614 Table titles:

615 Table 1. Selected physical properties of GAC, GAC-Fe_3O_4 and PAC.

616 Table 2. Kinetic parameters at different concentration for adsorption of DD by using DSRA
617 and GAC-Fe_3O_4 composite.

618

619 Figure Captions

620 Fig. 1. Saturation magnetization of GACs and PAC-Fe_3O_4 composites measured by SQUID.

621 Fig. 2. X-ray powder diffraction (XRD) patterns of the GAC-Fe_3O_4(B) and PAC-Fe_3O_4(A)
622 composites along with reference reflections for magnetite Fe_3O_4.

623 Fig. 3. Scanning electron microscopy (SEM) images of (a) DSRA (120X magnitude); (b)
624 DSRA (500X magnitude); (c) DSRA (800X magnitude); (d) GAC-Fe_3O_4 composite
625 (50000X magnitude); (e) GAC-Fe_3O_4 composite (150000X magnitude); and (f) GAC-
626 Fe_3O_4 composite (350000X magnitude).

627 Fig. 4. Batch equilibrium sorption isotherms of dibenzo-p-dioxin (DD) on GAC (black
628 squares) and GAC-Fe_3O_4(B) (red circles). Conditions: T=298 K, solution volume=30
629 mL, adsorbent =2.5 mg, contact time=10-48 h.
630 Fig. 5. Sorption kinetics of dibenzo-p-dioxin (DD) uptake by GAC and GAC-Fe_3O_4(B) over
631 40 h of contact. Top figure shows results from initial concentration of 0.8 mg/L,
632 middle figure shows results from initial concentration of 0.4 mg/L, and lower figure
633 shows initial concentration of 0.18 mg/L. GAC is represented by black squares and
634 GAC-Fe_3O_4(B) is represented by red circles. Conditions: T=298 K, solution
635 volume=30 mL, adsorbent =2.5 mg.
636 Fig. 6. Sorption kinetics of dibenzo-p-dioxin (DD) uptake by GAC, GAC-Fe_3O_4(B), PAC and
637 PAC-Fe_3O_4(A) over 18 h of contact. PAC is represented by black squares, PAC-
638 Fe_3O_4(A) is represented by solid red circles, GAC is represented by open black
639 squares, and GAC-Fe_3O_4(B) is represented by open red circles. Conditions: T=298 K,
640 solution volume=30 mL, adsorbent =2.5 mg. Conditions: DD concentration=0.8
641 mg/L, T=298 K, solution volume=30 mL, adsorbent=2.5 mg, contact time=1 h.
642

Figure Captions

Fig. 1. Saturation magnetization of GACs and PAC-Fe_3O_4 composites measured by SQUID.

Fig. 2. X-ray powder diffraction (XRD) patterns of the GAC-Fe_3O_4(B) and PAC-Fe_3O_4(A) composites along with reference reflections for magnetite Fe_3O_4.

Fig. 3. Scanning electron microscopy (SEM) images of (a) DSRA (120X magnitude); (b) DSRA (500X magnitude); (c) DSRA (800X magnitude); (d) GAC-Fe_3O_4 composite (50000X magnitude); (e) GAC-Fe_3O_4 composite (150000X magnitude); and (f) GAC-Fe_3O_4 composite (350000X magnitude).

Fig. 4. Batch equilibrium sorption isotherms of dibenzo-p-dioxin (DD) on GAC (black squares) and GAC-Fe_3O_4(B) (red circles). Conditions: T=298 K, solution volume=30 mL, adsorbent =2.5 mg, contact time=10-48 h.

Fig. 5. Sorption kinetics of dibenzo-p-dioxin (DD) uptake by GAC and GAC-Fe_3O_4(B) over 40 h of contact. Top figure shows results from initial concentration of 0.8 mg/L, middle figure shows results from initial concentration of 0.4 mg/L, and lower figure shows initial concentration of 0.18 mg/L. GAC is represented by black squares and GAC-Fe_3O_4(B) is represented by red circles. Conditions: T=298 K, solution volume=30 mL, adsorbent =2.5 mg.

Fig. 6. Sorption kinetics of dibenzo-p-dioxin (DD) uptake by GAC, GAC-Fe_3O_4(B), PAC and PAC-Fe_3O_4(A) over 18 h of contact. PAC is represented by black squares, PAC-

Fe_3O_4(A) is represented by solid red circles, GAC is represented by open black squares, and GAC-Fe_3O_4(B) is represented by open red circles. Conditions: T=298 K, solution volume=30 mL, adsorbent =2.5 mg. Conditions: DD concentration=0.8 mg/L, T=298 K, solution volume=30 mL, adsorbent=2.5 mg, contact time=1 h.

Figure 1

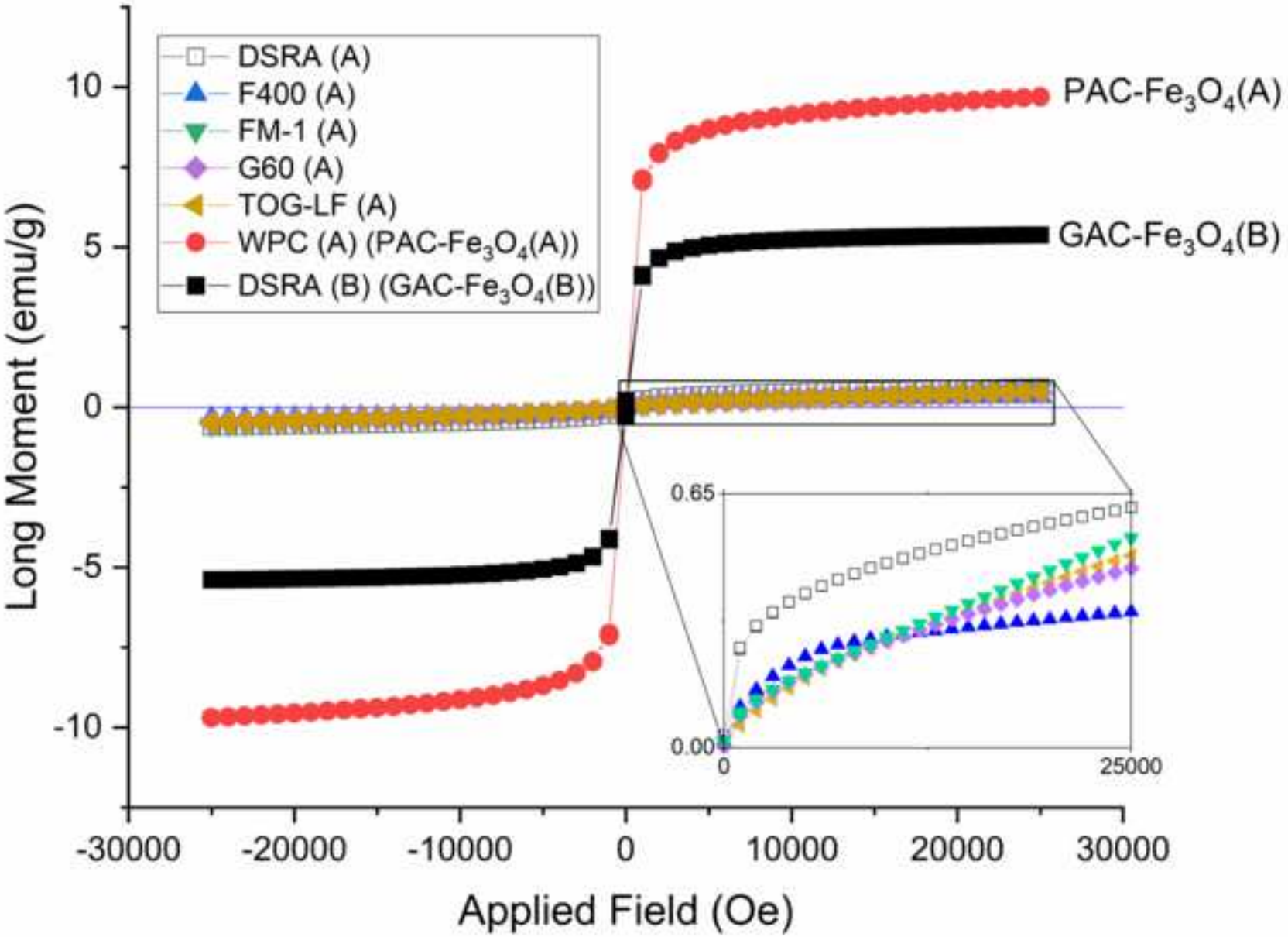

Figure 2

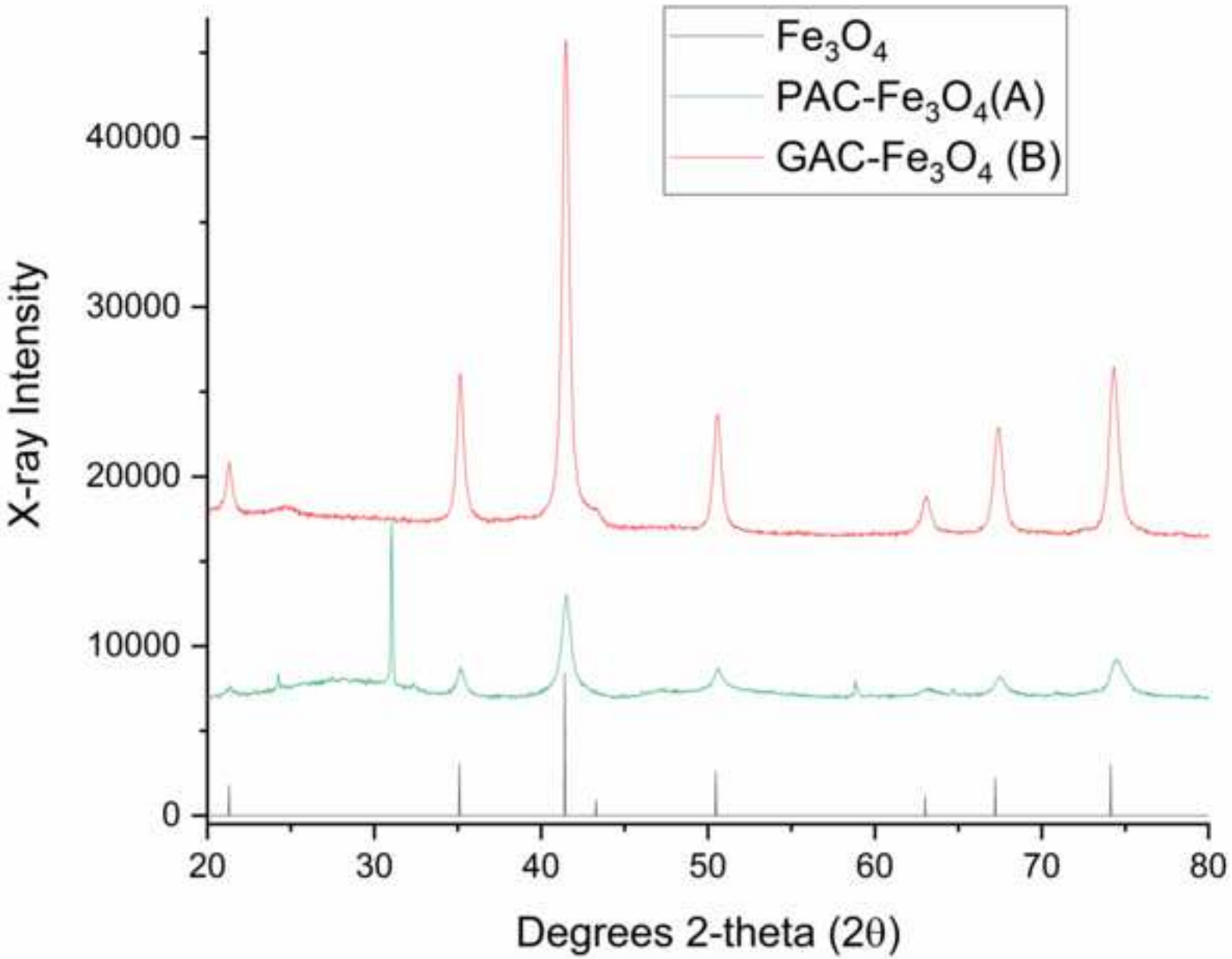

Figure 3

Click here to access/download;Figure;Figure 3 CHEM73363.tif

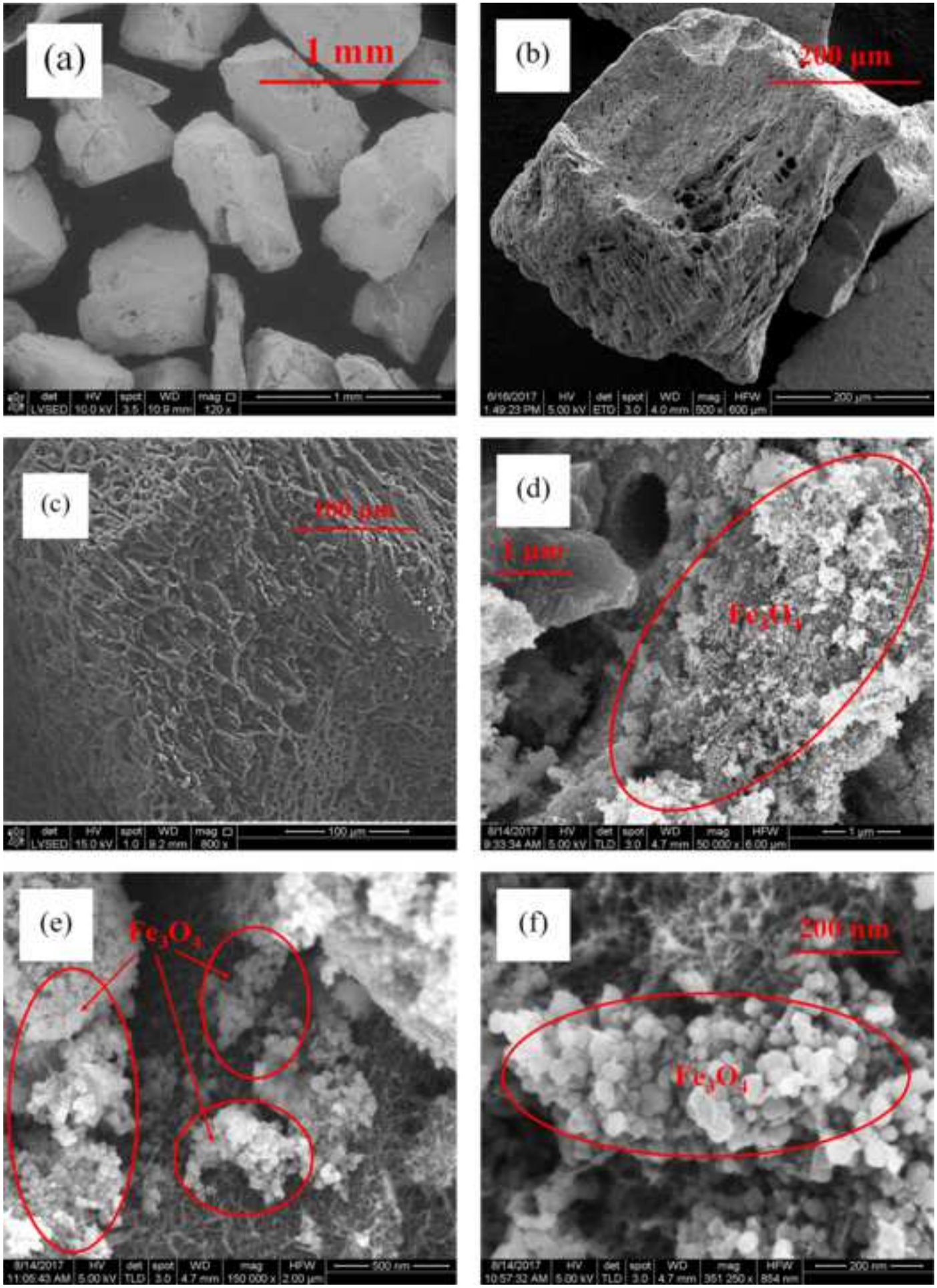

Figure 4

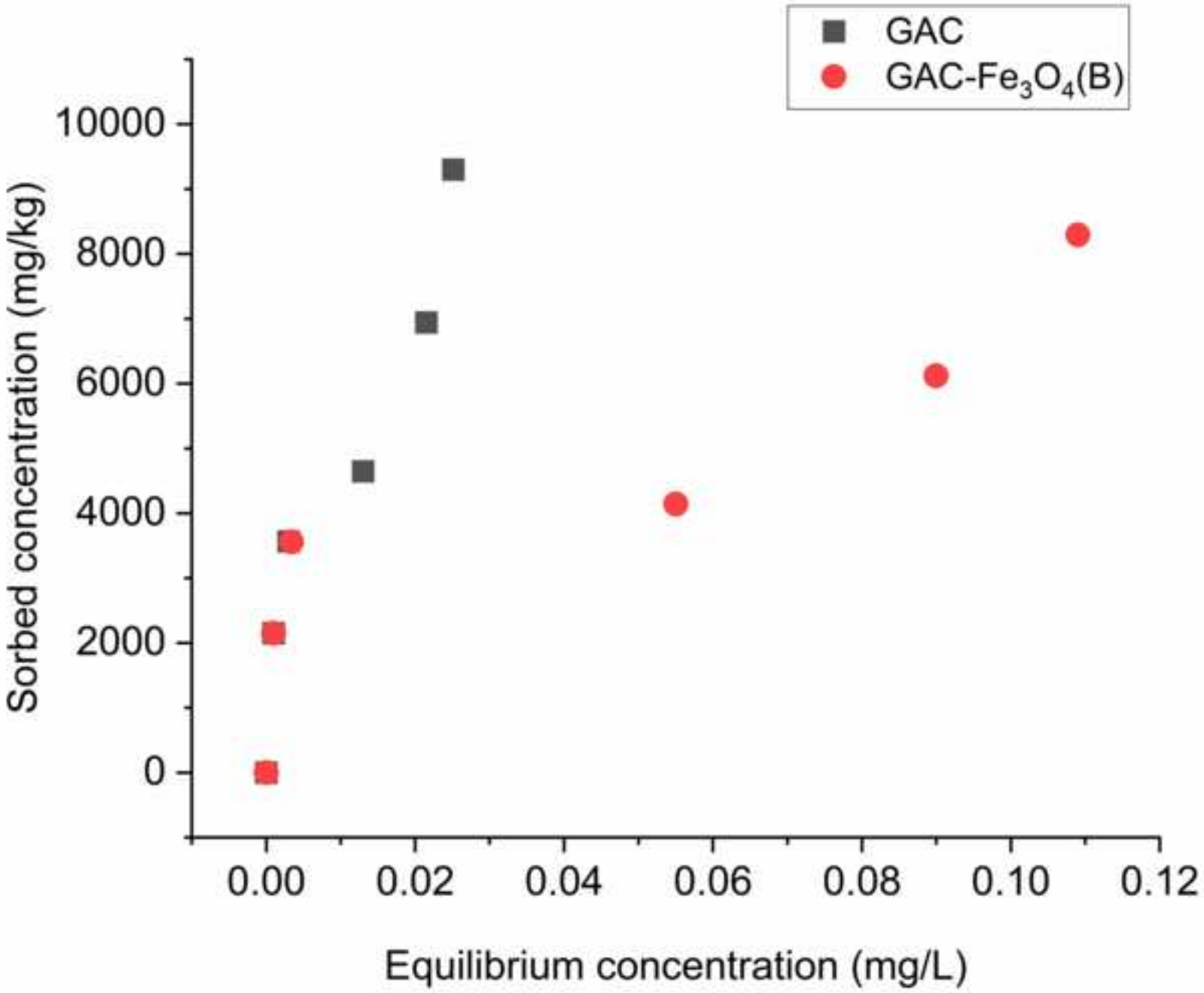

Figure 5

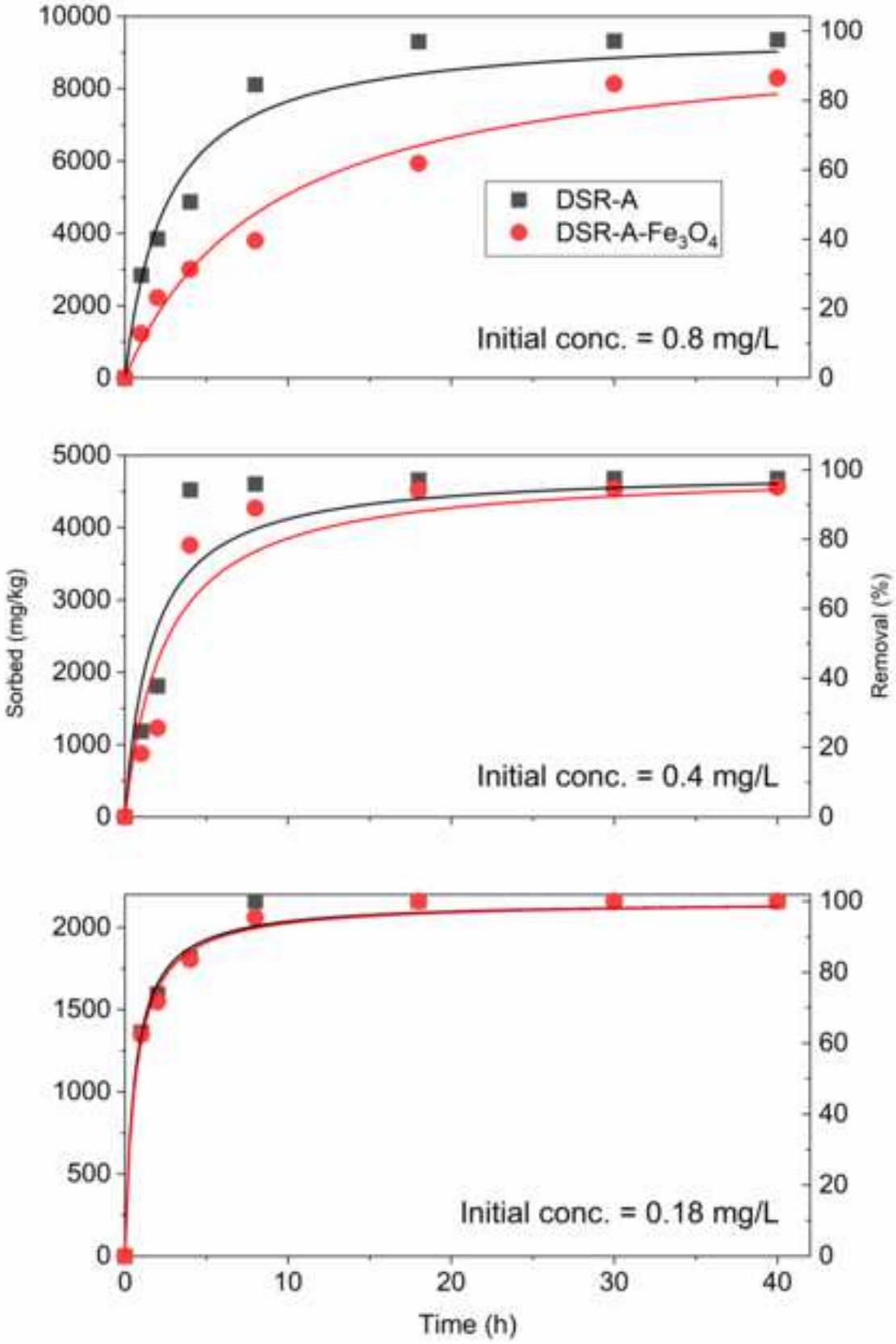

Figure 6

Click here to access/download;Figure;Figure 6 CHEM73363.tif

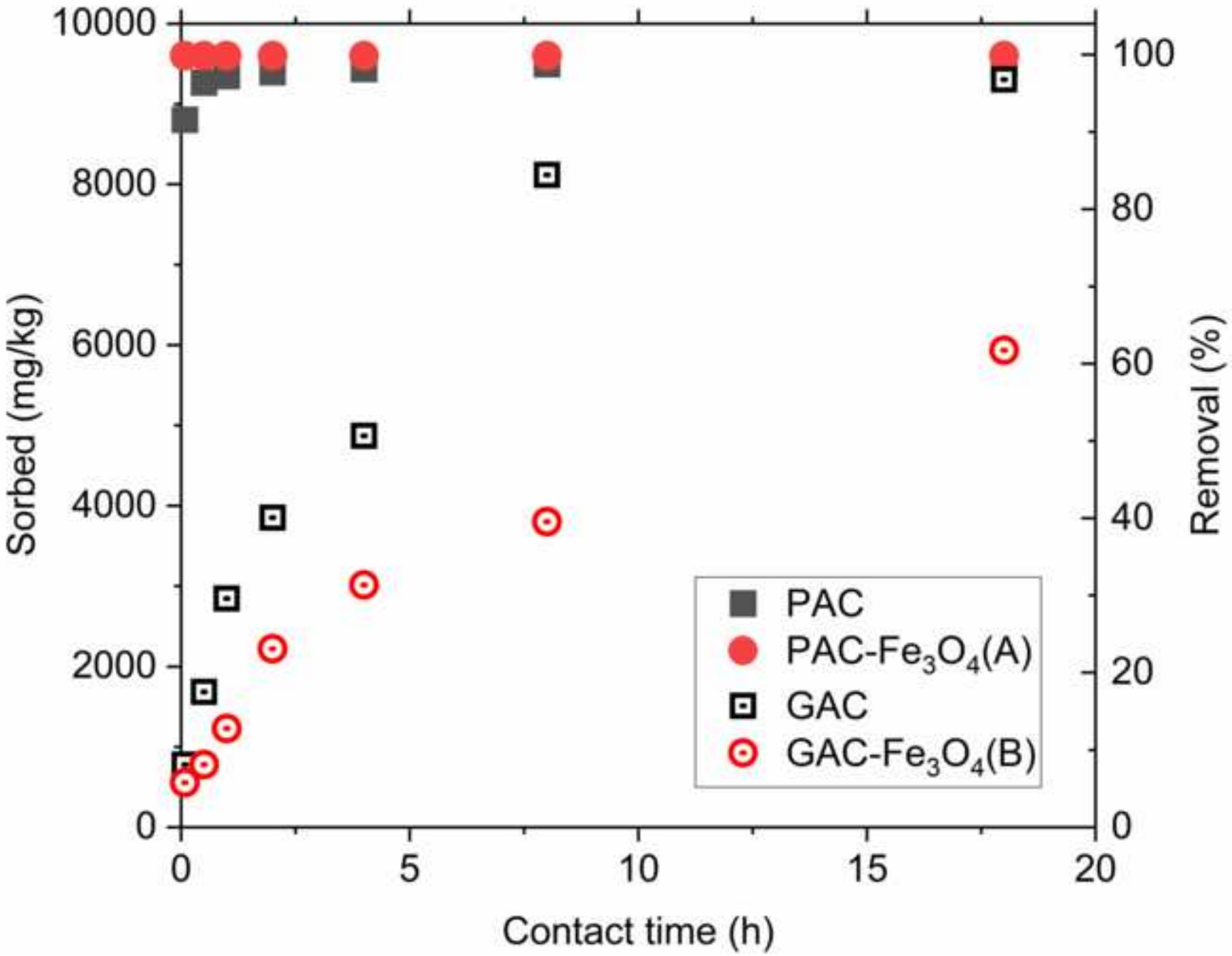

Table 1. Selected physical properties of the activated carbon materials

Material	Supplier	Source	Surface Area (m^2/g)	Mesopore vol. g/cc (% of total)	Micropore vol. g/cc (% of total)	[a]Magnetization after Syn. Method A (emu/g)	[b]Magnetization after Syn. Method B (emu/g)
G60	Cabot	Lignite	987	0.38 (57%)	0.29 (43%)	0.46	
FM-1	Cabot	Lignite	520	0.36 (71%)	0.15 (29%)	0.54	
TOG-LF	Calgon	Coal	916	0.15 (33%)	0.30 (67%	0.49	
F-400	Calgon	Coal	1044	0.16 (31%)	0.36 (69%)	0.35	
WPC (AC)	Calgon	Coconut	802	0.03 (9%)	0.29 (91%)	9.7	
DSRA (GAC)	Calgon	Pool Rej.	822	0.11 (22%)	0.38 (78%)	0.61	
DSRA-Fe_3O_4	Calgon	Pool Rej.	633	0.06 (18%)	0.26 (82%)		5.38

Note:

[a]: Magnetization after Fe_3O_4 impregnation at conditions of 338 K and 0.01 M $FeSO_4$.

[b]: Magnetization after Fe_3O_4 impregnation at conditions of 298 K and 0.1 M $FeSO_4$.

Table 2. The pseudo-second order kinetic model for GAC (DSRA) and GAC-Fe_3O_4(B)

	GAC (DSRA)			GAC-Fe_3O_4 (B)		
	q_e	k_2	Adjusted R Square	q_e	k_2	Adjusted R Square
0.18 mg/L	2160	7.62E-04	0.990	2160	7.02E-04	0.994
0.4 mg/L	4800	1.26E-04	0.893	4800	8.47E-05	0.916
0.8 mg/L	9600	4.10E-05	0.967	9600	1.17E-05	0.973